Journal of The Electrochemical Society

A Study of Graphite as Anode in the Electro-Deoxidation of Solid UO_2 in LiCl-Li_2O Melt

A Study of Graphite as Anode in the Electro-Deoxidation of Solid UO_2 in LiCl-Li_2O Melt

T. Biju Joseph, N. Sanil, K. S. Mohandas,[z] and K. Nagarajan

Fuel Chemistry Division, Chemistry Group, Indira Gandhi Centre for Atomic Research, Kalpakkam, 603 102, Tamil Nadu, India

Electrochemical behavior of graphite in LiCl and LiCl melts containing up to 1 wt% Li_2O was studied by using cyclic voltammetry and electrolysis, in the context of its probable use as anode in the electrochemical reduction of solid UO_2 in the molten salt at 650°C. The lithium deposition and chlorine evolution potentials of LiCl melt were determined by CV of tantalum (cathodic polarization) and graphite (anodic polarization) working electrodes as −2.19 V and +1.21 V vs Ni/NiO reference electrode respectively. In LiCl-Li_2O melts, carbon dioxide was formed on the graphite WE from > +0.75 V onwards and its current and potential range of formation increased with increase in the Li_2O content of the melt. Cathodic polarization of a UO_2 disc WE in LiCl-1 wt% Li_2O melt showed that the reduction of UO_2 to U occurs at −2.18 V and the lithium metal deposition on it at −2.36 V. Electro-reduction experiments carried out with a dense UO_2 pellet cathode and graphite anode in both LiCl and LiCl-Li_2O melts proved that the surface of the pellet was reduced to U metal at ≥ −2.2 V. The reduction became increasingly difficult with increase in the Li_2O content of the melt.
 [DOI: 10.1149/2.0521506jes]

Manuscript received November 20, 2014. Published March 10, 2015.

Nuclear energy is considered as a major source of electricity for the present and future demands of the modern world. Sodium cooled fast reactor with metal fuel is proposed as one of the future reactor systems in the Generation IV concept and such reactors are considered to be inherently safe, economically viable and resistant to nuclear proliferation.[1] U-Pu-Zr alloy is used as the metal fuel and hence production of these metals is of importance in the context of nuclear electricity. These metals have been produced from their oxides by the conventional chemical processes for the past several decades and there has been a great deal of interest to develop more efficient methods of production of the metals directly from the oxides.

Spent metal fuels are reprocessed by pyrometallurgical process, in which the major and minor actinides are recovered by an electrorefining process carried out in a molten bath of LiCl-KCl at 500°C.[2] Most of the nuclear reactors use uranium oxide and mixed oxide of uranium and plutonium (MOX) as the fuel and the spent fuel containing UO_2 and PuO_2 along with other oxides and fission products can be processed to obtain U and Pu for preparation of metal fuel. Reprocessing of spent oxide fuels by the molten salt electrorefining process is difficult as the oxides do not dissolve in the molten chlorides. Hence an intermediate process is required to convert the spent-oxide fuel to a metal form, which can be subsequently electrorefined to separate the actinides of interest. Chemical reduction of the spent oxide fuel by lithium metal in molten LiCl at 650°C was reported in this context.[3] The process required handling of large quantities of highly reactive lithium metal. The process also demanded frequent change of the molten bath due to build up of Li_2O and hence the use of large quantities of the molten salt. Obviously these factors raise issues of safety of handling and storage of hygroscopic salt and highly irradiated fuel material. In this context the direct oxide electrochemical reduction (DOER) process discovered recently has attracted attention.[4,5]

In this process the solid metal oxide (eg. UO_2), configured as the cathode, is directly converted to the metal (U) by solid state electrolysis in a suitable molten salt medium like LiCl or $CaCl_2$. Generally platinum or graphite is used as the anode in the electro-reduction process. During electrolysis, the oxygen present in the metal oxide cathode is liberated as O^{2-} ions and are discharged at the anode as either O_2 (on platinum anode) or as carbon oxides (on graphite anode). Small quantities of the respective oxides are added to the electrolyte melt to ensure the presence of O^{2-} ions in the melt, which play an important role as the bridge to transport the cathodically generated O^{2-} ions across the cell. The reactions taking place in a typical electro-reduction cell with UO_2 as the cathode and platinum or graphite as the anode can be written as follows.

$$UO_2 + 4e^- \rightarrow U + 2O^{2-} \quad [1]$$

$$2O^{2-} \rightarrow O_2 + 4e^- \quad \text{Pt anode} \quad [2]$$

$$O^{2-} + C \rightarrow CO + 2e^- \quad \text{graphite anode} \quad [3]$$

$$2O^{2-} + C \rightarrow CO_2 + 4e^- \quad \text{graphite anode} \quad [4]$$

The electro-reduction process carried out in $CaCl_2$ melt or melts containing $CaCl_2$ and with graphite anode is known as 'FFC Cambridge process'.[5,6] Reaction 4 takes place predominantly on a graphite anode working at low current densities.

Uranium dioxide is the major constituent of the spent oxide fuel and therefore several studies have been reported on the electrochemical reduction of solid UO_2.[7–13] Almost all such studies have been carried out in LiCl melts containing 1–3 wt% Li_2O at 650°C with platinum anode. The low melting temperature of LiCl (605°C) and the high reducing power of lithium favored the use of lithium chloride as the electrolyte. Platinum became the anode of choice in the nuclear work probably due to its perceived inert nature in the melt, which enables maintenance of a clean molten salt bath and hence the possibility of efficient production of pure U metal in the melt. Graphite on the other hand is known to make the electrolyte melt dirty with carbon particles. It could also make problems for electrolysis by generation of carbonate ions and their recycling with adverse effect on the current efficiency.[5] However, though platinum was considered as an inert electrode in the LiCl-Li_2O melt, many studies, of late, have proved that it is not so.[13–17] It has been established that platinum anodically reacts with the oxide ions present in the electrolyte melt to form Li_2PtO_3 as per the reaction

$$2Li^+ + Pt + 3O^{2-} \rightarrow Li_2PtO_3 + 4e^- \quad [5]$$

The reaction leads to corrosion of the electrode and in its eventual physical loss.

Platinum is a very precious metal and it will be uneconomical to use the costly metal as a consumable anode in large-scale electro-reduction cells. There have been many efforts to develop oxygen gas evolving inert anodes for electrolysis of oxides in molten chlorides, but none reported successful for a commercial scale operation till date.[18–22] On the other hand graphite, notwithstanding the problems mentioned previously, is a widely accepted anode material of choice for molten salt electrolysis due to its cheapness, easy availability, machinability etc.. It has been the proven anode in the electrolysis of molten chlorides

[z]E-mail: ksmd@igcar.gov.in

(eg. Na production from NaCl) and also oxide (Al production by Hall-Heroult process) and could possibly serve as a good anode in the molten salt electro-deoxidation cells too, provided the problems associated with its use are addressed and sorted out. In this context, it is important to mention that graphite has been successfully used in the electro-reduction cells in the "FFC Cambridge process' for production of sizeable quantities of titanium metal (3 kg) from titanium oxide.[23] All these make it sensible to think of exploring the possibility of using graphite as anode in the electrochemical reduction of UO_2 in LiCl-Li_2O melts.

Two articles have been published on the subject recently.[24,25] Both the articles give a good account of the theoretical aspects of the graphite anode reactions in the LiCl-Li_2O melts and some experimental evidence to support the theory. The feasibility of using graphite in the electrochemical reduction of UO_2 has been discussed in Ref. 25. Also there have been some reports on the anodic behavior of carbon in $CaCl_2$-CaO melts.[26,27] Recently Takenaka et al.[28] reported a study on the anodic behavior of graphite in KCl-LiCl-Li_2O melts at 425°C and Tunold et al.[29] on the anodic behavior of graphite and vitreous carbon in molten NaCl-$CaCl_2$-CaO system.

We have been studying the electro-reduction behavior of uranium oxides to uranium metal in LiCl-Li_2O melt with platinum anode and parallely examining the feasibility of using graphite as the anode in the cell and the fundamental issues thereon. In this regard we have carried out cyclic voltammetry experiments to study the electrochemical behavior of graphite and solid UO_2 electrodes in LiCl-(0-1) wt% Li_2O melts at 650°C and the results have been directly correlated to the electrochemical reduction behavior of UO_2 by constant voltage electrolysis. It is important to mention here that the anodic reactions of graphite obtained by the CV measurements and reported in both Refs. 24 and 25 do not match with the results of our study. The reported results also seem to be inconsistent with the corresponding data of the UO_2 electro-reduction cell.[25] For instance, the anodic CO/CO_2 evolution reaction, based on the CV results in Refs. 24 and 25, should take place at $\sim +1.5$ V vs Li/Li^+ but the actual anode potential of the UO_2 electro-reduction cell in Ref. 25 was observed to be higher by ~1 V. The interpretation of the anodic reaction potentials of the CV in the two articles, especially that of the governing reaction of CO/CO_2 formation on the graphite electrode appeared to be flawed. We, therefore, have made attempts to re-interpret the data in the light of the results of our study. For the sake of comparison, the potentials referred to different reference electrodes in these articles and also the relevant data of the present study have been normalized to Li^+/Li scale with the available data in the respective articles. The relevant results of the study are reported in detail in this article.

Experimental

LiCl (99.99% purity, Alfa Aesar) was vacuum dried at 150°C for 24 h prior to use in the experiment. Approximately 280 g of the salt was loaded in alumina crucible. The loading of salt in the reactor vessel and subsequent assembly of the cell with all the electrodes in place were carried out in an argon atmosphere glove box having purity better than 5 ppm of O_2/H_2O. After assembling, the cell was taken out of the glove box and heated to 650°C with the help of an electrical resistance furnace. Purified argon gas was purged continuously through the reactor. Pre-electrolysis of the molten salt was carried out at 3.1 V for 8 h and thereafter CV of tantalum, graphite and UO_2 disc electrodes were recorded in the melt. A 1.2 mm dia. tantalum wire with ~ 2 mm of its tip dipping in the melt was used as working electrode for cathodic polarization and a graphite rod (10 mm dia. × 100 mm long, density 1.85 g/cc and supplied by M/s Nickunj Group, Mumbai) with an area of 1 cm^2 immersed in melt as the WE for anodic polarization. UO_2 pellets (14.3 mm dia. with 2 mm dia. hole at the centre, 8 mm thick, 95% TD, supplied by AMD, Hyderabad) were sliced to thin circular discs weighing 2–4 g and were used as the working electrode in CV studies and also as the cathode in the electro-reduction experiments. In all the cells, the discs were connected to a tantalum wire, which also served as the current lead to the oxide electrode. For CV measurements, the tantalum wire was inserted through the central hole of the UO_2 disc and tied to it tightly. In order to provide more electrical connection points to the electrode, the UO_2 disc used in the electro-reduction experiments were wrapped around with the tantalum wire. UO_2 discs of 13 mm dia. and without a central hole, prepared by powder compaction and sintering (1550°C/2.5 h) were also used in few experiments. For CV measurements, the edge of the UO_2 disc electrode was only allowed to touch the electrolyte melt whereas the disc along with the tantalum lead wire was fully immersed in the melt during the electro-reduction experiments. A 10 mm dia., 100 mm long graphite rod was used as the counter electrode in the electrolytic experiments. A Ni/NiO couple, made by placing a Ni wire in contact with NiO powder contained in a one-end-closed alumina tube with a pinhole at the bottom, was used as the reference electrode in both CV measurements and during electrolysis.[30] The potential of the electrode was found to be stable within ±1 mV for about 30 minutes in the LiCl-Li_2O melt and this was good enough for the CV measurements. The electrode potential was observed to change marginally (10–15 mV) during long term exposure (25 h and above) in the melt in electro-reduction cells. The half cell potentials of the electro-reduction cells measured over a long period of time were not expected to be very accurate and hence the small instability of the electrode was acceptable.

Weighed quantities of Li_2O (99.5% purity, Alfa Aesar) was added to the pre-electrolysed and solidified LiCl salt, which on melting gave the desired LiCl-Li_2O melt composition for different experiments. The CV measurements, as mentioned above for LiCl melt, were repeated in the LiCl-Li_2O melts too. Cyclic voltammetry was performed using a potentiostat/galvanostat (AUTOLAB PGSTAT 30). Electrolysis of UO_2 discs was carried out at a constant voltage of 3.2 V in both LiCl and LiCl-Li_2O melts. The graphite anode and UO_2 disc cathode potentials during electrolysis were monitored with the Ni/NiO reference electrode. Measurements, acquisition and storage of all electrical data were accomplished with the help of a data acquisition/switch unit (AGILENT 34970 A).

After the electrolysis, all the electrodes were lifted out of the melt to the upper, cooler portion of the cell and cooled to room temperature under flow of argon gas. The cooled cell was opened inside the glove box to retrieve the electrolysed product. The salt adhering to the cathode was physically removed and the electrolysis product was subjected to XRD analysis (PHILIPS xPERT diffractometer with Cu-Kα radiation) without exposure to the ambient air. This was done by covering them in a protective organic film so that the originality of the reaction products could be maintained during the XRD measurements. Some of the samples were also washed with water or ethanol before the XRD analysis. The microstructures of the freshly fractured surface of the samples were taken with a Philips model XL30 scanning electron microscope.

The potentials measured against Ni/NiO reference electrode in this work, wherever necessary, have been converted to the Li^+/Li scale with the help of Li^+/Li potentials of the respective melts determined by CV measurements.

Results and Discussion

Cyclic voltammetry of tantalum and graphite in LiCl melt.— The cyclic voltammograms obtained during cathodic polarization of tantalum and anodic polarization of graphite in pre-electrolysed LiCl melt are given in Fig. 1a and Fig. 1b respectively. The steep increase of currents on the tantalum WE at potentials negative to −2.1 V and on the graphite WE at potentials positive to +1.2 V are due to the lithium metal deposition ($Li^+ + e \rightarrow Li$) and chlorine evolution ($Cl^- \rightarrow 1/2Cl_2 + e^-$) reactions respectively. The precise potentials of the two reactions w.r.t the Ni/NiO reference electrode were determined by extrapolation of the straight line portion of the plot to zero current as −2.19 V and +1.21 V respectively. The electrochemical window of LiCl was thus deduced as 3.40 V. This value was found to be in good agreement with the reversible decomposition potential of the melt, deduced from the Gibbs energy of formation for LiCl at 650°C ($\Delta_f G^\circ$

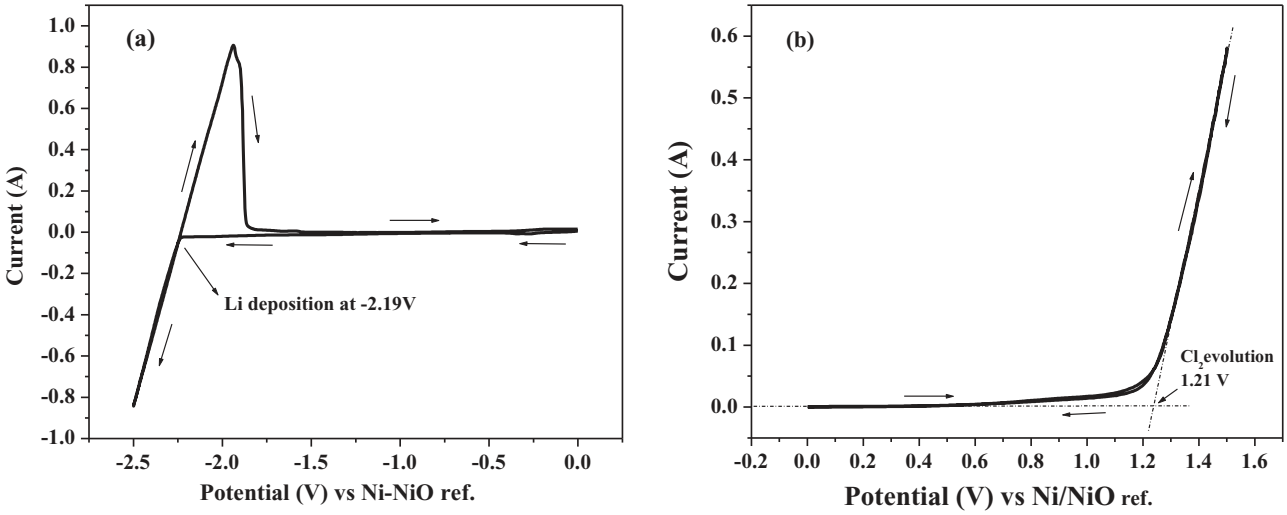

Figure 1. Cyclic voltammograms of (a) tantalum (area: 0.086 cm^2) and (b) graphite (area: 1 cm^2) working electrodes in LiCl melt at 650°C. Scan rate: 50 mV/s.

$LiCl_{923K}$ = 333.8 kJ/mol., $E_{d\ (LiCl)}$ = 3.46 V).[31] The closeness of the theoretical and measured potentials confirms that the chlorine evolving graphite anode is inert in the melt and has insignificant overvoltage to chlorine evolution.

Cyclic voltammetry of tantalum and graphite in LiCl-Li_2O melts.— The CVs of a tantalum working electrode (1.2 mm dia. wire, length of immersion 2 mm) upon cathodic polarization and a graphite working electrode (1 cm^2) upon anodic polarization in LiCl melts containing 0.1, 0.5 and 1.0 wt% Li_2O are shown in Fig. 2a and Fig. 2b respectively. The background current of the CVs of the tantalum electrode and the Li^+/Li potentials of the melts increased marginally with increase in the Li_2O content of the the melts. The shift in the Li^+/Li potentials may be related to the small change in the Li_2O concentrations of the melts and/or to the marginal instability of the reference electrode. Though the change in the Li^+/Li potentials was very small, the CVs of the graphite working electrode in these melt compositions showed marked difference in potentials and shapes compared to that of the pure LiCl melt. These features became more and more prominent as the Li_2O content in the melt was increased. During the forward scan, a significant increase of current was noticed from ~ +0.75 V in all the three melts. The current increased linearly with the applied voltage to a maximum value before registering a decrease. The magnitude and potential window of the current too increased with increase in the Li_2O content of the melt. The current was attributed to the reaction $C + 2O^{2-} \rightarrow CO_2 + 4e^-$. Further polarization of the electrode towards higher anodic potentials showed the onset of a different anodic reaction whose current again increased linearly with the applied potential. The current was attributed to the chlorine evolution on the graphite electrode as per the reaction, $2Cl^- \rightarrow Cl_2\ (g) + 2e^-$. The chlorine evolution potential was observed to shift to higher anodic potentials with increase in the Li_2O content of the melt. Similar kind of anodic behavior noticed on platinum anode has been reported in our previous article.[17] The potential window of the LiCl-1 wt%. Li_2O melt for CO_2 formation was found to be 1.0 V (+ 0.75 to + 1.7 V) beyond which the chlorine evolution took place on the graphite electrode. The wide potential window of CO_2 formation is considered a desirable feature of the electrolyte melt as it allows the reduction process to be conducted without chlorine gas evolution at the anode. Chlorine evolution is an undesirable anodic reaction as it decomposes the electrolyte melt and causes corrosion of the cell components and creates operational and safety problems.

The results of the CV of graphite electrode in LiCl-1wt.% Li_2O melt, reported in Refs. 24 and 25 can now be compared with those of this study. The CV patterns given in Ref. 24 show an anodic current wave starting at ~ +1.5 V and the other at ~ +2.8 V vs Li^+/Li. Two anodic waves, one at +1.595 V and the other at +2.996 V have been shown in the CV patterns of Ref. 25. The authors of both the articles have assigned the first current wave of the CVs to the formation of CO_2 gas as per the reaction $C + 2O^{2-} \rightarrow CO_2 + 4e^-$, which should take place thermodynamically at +1.44 V vs Li^+/Li under standard conditions of the reactants and products at 650°C.[31] The rapidly rising

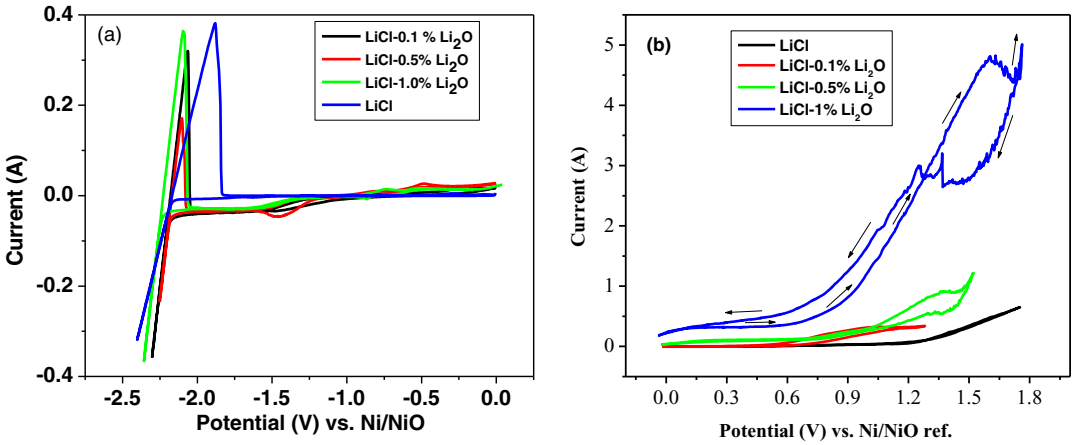

Figure 2. CV traces of (a) tantalum and (b) graphite working electrodes in LiCl-Li_2O melts with different concentrations of Li_2O. Scan rate: 50 mV/s.

second current at +2.8 V of CV in Ref. 24 has been related to the evolution of O_2 gas on the electrode and the reaction responsible for current at +2.996 V in the CV shown in Ref. 25 is reportedly 'could not be identified'. While the first current wave was not identified in our study, the wave starting at ∼+0.75 V vs Ni/NiO reference (+2.94 V vs Li^+/Li) has been assigned to formation of CO_2 gas. It will be seen in later sections of this article that the graphite anode potential remained always at ∼ +3.0 V vs Li^+/Li during electro-deoxidation of the UO_2 electrode in LiCl-1wt.% Li_2O melt and the anode was corroded by formation of CO_2 gas, which subsequently dissolved in the electrolyte melt to generate significant amounts of CO_3^{2-} ions. These results confirm that the CO/CO_2 evolution on the graphite anode in LiCl-1wt.% Li_2O do take place at ∼+3.0 V and not at ∼+1.5 V as interpreted in Refs. 24 and 25. Sakamura et al.[12] have studied the anodic behavior of glassy carbon in LiCl-(0-0.13) mol.% Li_2O melts and reported a current wave starting at ∼+1.9 V vs Li^+/Li, which was suggested to be due to the formation of CO_2 on the electrode. Though the current wave below +2.0 V in the CVs in these articles[12,24,25] are referred to the anodic formation of CO_2 gas, no evidence to support this interpretation has been provided. However, Mohammedi et al.[26] and Tunold et al.[29] reported the existence of an adsorption reaction $O^{2-} + xC \rightarrow C_xO_{(ads)} + 2e^-$ taking place on the electrode at anodic potentials cathodic to CO_2 formation. It is highly likely that the current waves starting at +1.5 V in Refs. 24 and 25 and at 1.9 V in Ref. 12 are due to the adsorption of O^{2-} on the active surface sites of the high surface graphite anode and not due to the CO/CO_2 formation on the electrode. The adsorption takes place on the graphite anode over a potential range, beyond which the CO/CO_2 evolution commences on the electrode. Mohandas et al. have reported studies on the anodic adsorption of Cl^- ions on different forms of graphite in molten $NaAlCl_4$[32] and also O^{2-} ions on graphite anode during electro-reduction of TiO_2 in $CaCl_2$ melt.[33] Based on the facts presented above, it is highly likely that the anodic current starting at 2.996 V in the CV of LiCl-1 wt% Li_2O melt at 650°C[25] is due to formation of CO/CO_2. The high formation potential of CO_2 compared to the theoretical formation potential of +1.44 V indicates that the anodic process is associated with high overvoltage. The low concentration of the Li_2O (≤ 1 wt%) in the LiCl melt compared to the saturation solubility of 8.7 wt% at 650°C[34] can also be a factor contributing to the increase in the reaction potential.

Cyclic voltammetry of UO_2 pellet electrode in LiCl melt.— The cyclic voltammograms of the tip of a dense UO_2 pellet (95% TD, 14.3 mm dia., 3 mm thick) working electrode under cathodic polarization in LiCl melt are shown in Fig. 3 (curve a and curve b). The pellet was hung vertically from the top of the cell with the help of a tantalum wire in such a way that its edge just touched the top of the melt in the crucible. A 10 mm dia. graphite rod with 5 cm length of it dipping in the melt served as the counter electrode. The CV was recorded after allowing the pellet to remain in contact with the melt for 30 minutes. A current wave starting at −1.5 V and peaking at −2.4 V, positive to the lithium metal deposition at −2.5 V is assumed to be due to the reduction of UO_2 to U (the features are not prominent in Fig. 3 (curve a) due to the compressed scale of the y-axis). The pellet was subsequently allowed to remain in contact with the melt for 24 hours in the same configuration to improve wetting and the CV recorded thereafter is shown in Fig. 3 (curve b). The CV characteristics make it evident that the oxide pellet became electrochemically more active after immersing in the melt for a longer duration of time.

Three current waves a, b and c are visible on the CV during the forward cathodic sweep. 'a' and 'b' are considered to be due to the adsorption of lithium ions taking place on the active surface sites of the UO_2 electrode. The prominent current wave 'c' with the current starting at −1.78 V and peaking at −2.18 V can be attributed to the reduction of UO_2 to U. The steep increase of current with potential (d) seen at potentials negative to this obviously is due to the lithium deposition on the electrode, the reverse process of which is shown by the current hump (d*) in the reverse anodic sweep of the voltammogram. The $Li^+ + e \leftrightarrow Li$ potential is determined as −2.36 V. The anodic current wave 'e' at −1.25 V, most probably represents the oxidation of U metal to U^{4+}. The anodic waves 'f' and 'g' may be corresponding to the cathodic waves 'b' and 'a' respectively. A comparison of Fig. 1a and Fig. 3 (curve b) shows that the lithium deposition on the uranium oxide pellet takes place at a potential which is 170 mV negative to that on a tantalum electrode in the same melt. The negative shift of the lithium deposition potential of the UO_2 electrode may be due to its higher resistance and hence the higher IR drop of the oxide electrode. The potential separation of 180 mV between the UO_2 reduction (−2.18 V) and the lithium deposition (−2.36 V) in Fig. 3 (curve b) shows that the reduction of the electrode could be possible in the absence of the electro-generated lithium metal.

Cyclic voltammetry of UO_2 in LiCl-1 wt% Li_2O melt.— The CV of the tip of a high density UO_2 electrode, obtained under identical experimental conditions to that of the previous experiment, except the melt composition of LiCl-1 wt% Li_2O, is shown in Fig. 4. Prior to recording the CV, the UO_2 electrode was subjected to several cycling between 0.0 V and −2.3 V to make it electrochemically active. The

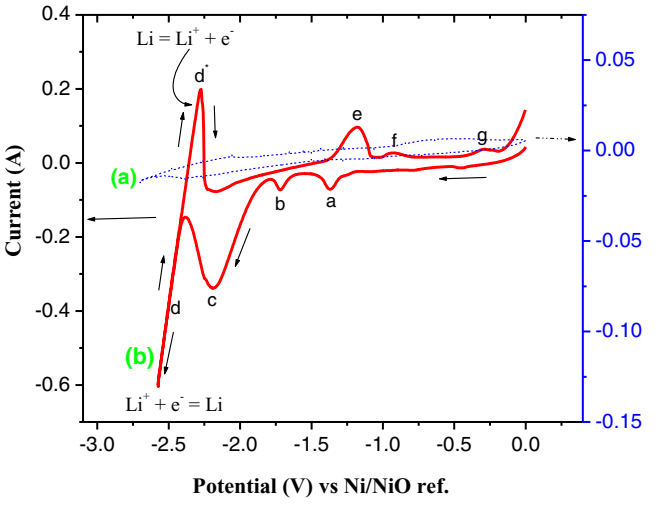

Figure 3. Cyclic voltammograms of the tip of a dense UO_2 pellet obtained in LiCl melt, (a) recorded after 30 minutes of immersion and (b) recorded after 24 hours of immersion in the melt. Scan rate: 25 mV/s.

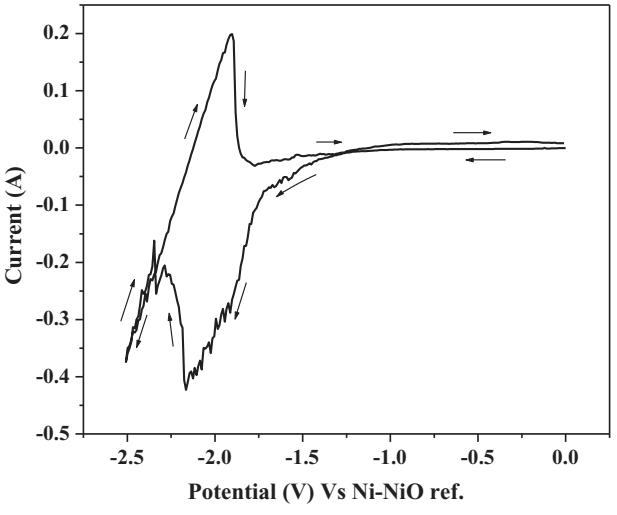

Figure 4. Cyclic voltammogram of a high dense UO_2 pellet obtained in LiCl-1wt.% Li_2O melt. The electrode was subjected to several potential cycles, within the potential limits of 0.0 V and −2.3 V, before recording the CV depicted. Scan rate: 25 mV/s.

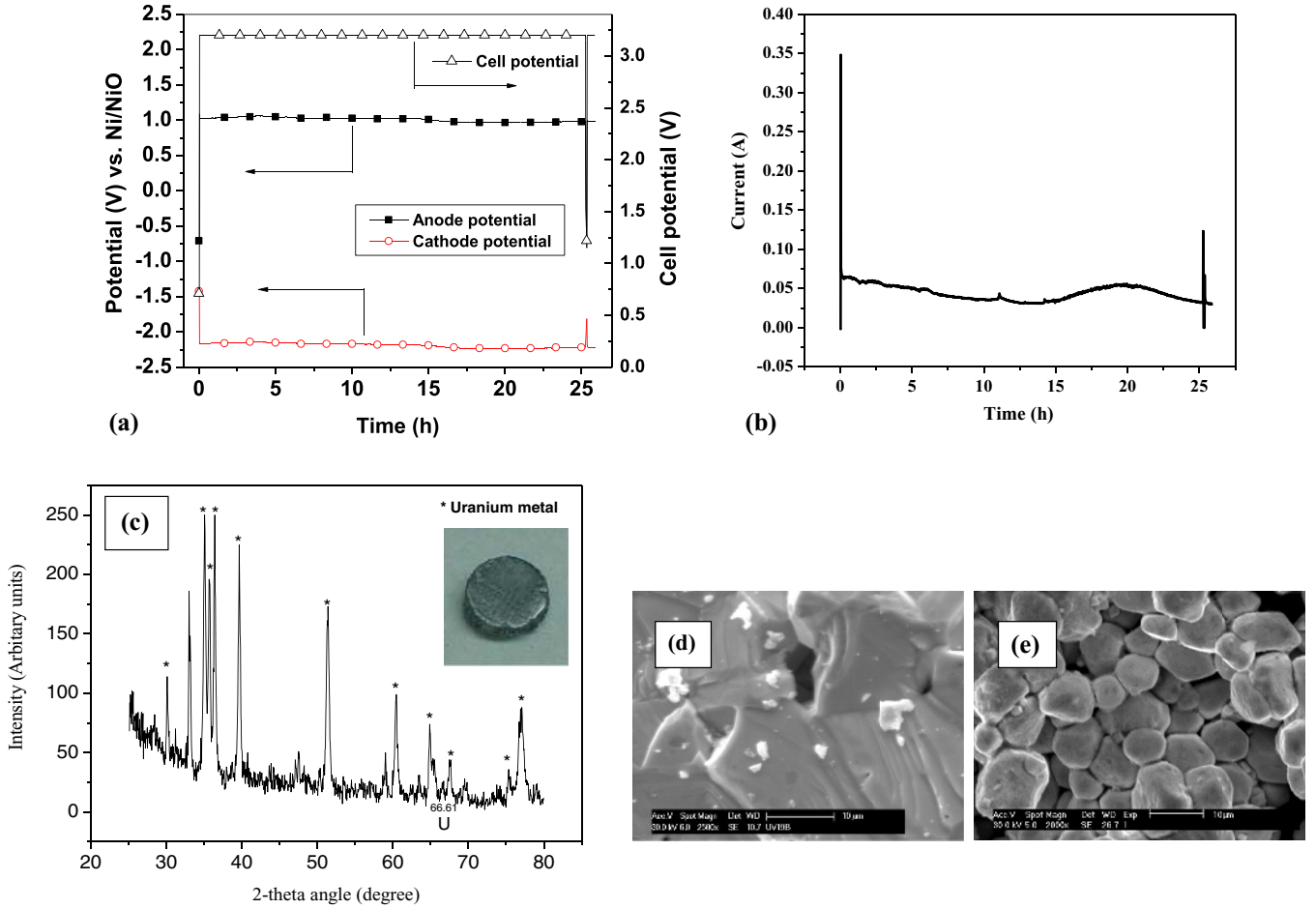

Figure 5. The variation of (a) half cell potentials and (b) current during constant voltage electrolysis of a UO_2 pellet in LiCl melt at 650°C at 3.2 V with graphite anode, (c) X-ray diffractogram of the polished surface of the electrolysed pellet. The photograph of the pellet is shown in the inset. The SEM image of the fractured surfaces of the original UO_2 pellet and its reduced surface metal layer are shown in (d) and (e) respectively.

CVs recorded before cycling resembled to that of a resistor and was devoid of any significant electrochemical features, which could be attributed to the reduction of the oxide. But the CV of the electrode shown in Fig. 4 shows that the UO_2 electrode did become electrochemically active by the repeated cycling between 0.0 V and −2.3 V vs Ni/NiO in the melt. From the CV it is evident that the electro-reduction of the UO_2 disc electrode occurred at −2.18 V and subsequent metal deposition on it at −2.36 V. The difference in the cathode potential for electro-reduction and lithium metal deposition strongly indicates the possibility of reduction of the electrode by electrons.

Studies on the electro-reduction of UO_2 pellets.— The variation of the half-cell potentials and current of an electro-reduction cell with a UO_2 pellet electrode (13 mm dia. × 2 mm thick, 2 g), immersed fully in the melt, as the cathode and a graphite rod as the anode in LiCl melt at 650°C, under a constant applied voltage of 3.2 V, is shown in Fig. 5a and 5b respectively. Immediately upon imposition of the potential to the cell, the oxide cathode assumed a potential of −2.15 V and the graphite anode ∼1.0 V. The potential of the cathode increased slowly toward a maximum value of −2.2 V and that of the anode to +0.95 V over a period of 25 h. It is interesting to note that the cathodic potential of the cell corresponded to that of the current wave 'c' in the CV shown in Fig. 3b, indicating thereby that the UO_2 electrode was undergoing electro-reduction to uranium metal. The potential of the graphite anode was only 1 V or less throughout the course of the experiment, which ruled out the possibility of chlorine gas evolution (1.21 V) on it. Graphite anode in molten chloride electrolysis is known to pass small currents at potentials negative to chlorine evolution potential (Fig. 1b) due to adsorption of chloride ions on its active surface sites.[29,33] Hence, in the present case, the anodic process sustaining the small cell current (∼50 mA), especially in the beginning stages of electrolysis, could be due to adsorption of the chloride ions. As electrolysis was continued, O^{2-} ions released from the UO_2 cathode could also be discharging on the anode as per reaction 4.

The current of a typical electro-reduction cell, working under constant applied voltage, decreases with time indicating thereby that the electrode is undergoing deoxidation. The current behavior of the present cell (Fig. 5b) is in agreement with this theory, except for a small increase of current toward the later part of electrolysis. However, the magnitude of the current was small compared to that noticed in similar electro-reduction experiments with oxide electrodes like TiO_2, Nb_2O_5 etc. The difference in the magnitude of currents may be attributable to the difference in the electro-active surface area of the electrodes in the melt. TiO_2 and Nb_2O_5 cathodes are reactive in the $CaCl_2$ /LiCl melts and form ternary insertion compounds (eg. Li_2TiO_3, $CaNb_2O_6$ etc.) whereas non-reactive UO_2 does not form such compounds.[35] The reactive nature of the former electrodes enables larger area of the electrodes to be electrochemically active, which in turn reflect in higher cell currents. Another reason for the small current on UO_2 electrode could have been its dense nature, which probably prevented penetration of the electrolyte melt to the interior parts of the pellet thus limiting the effective surface area for reaction. This would suggest that the pellet was undergoing reduction on its surface only where the necessary condition for electro-reduction, i.e. melt-oxide-electron three phase contact co-existed. The physical examination and XRD analysis of the electrolysed pellet agreed with this as the results

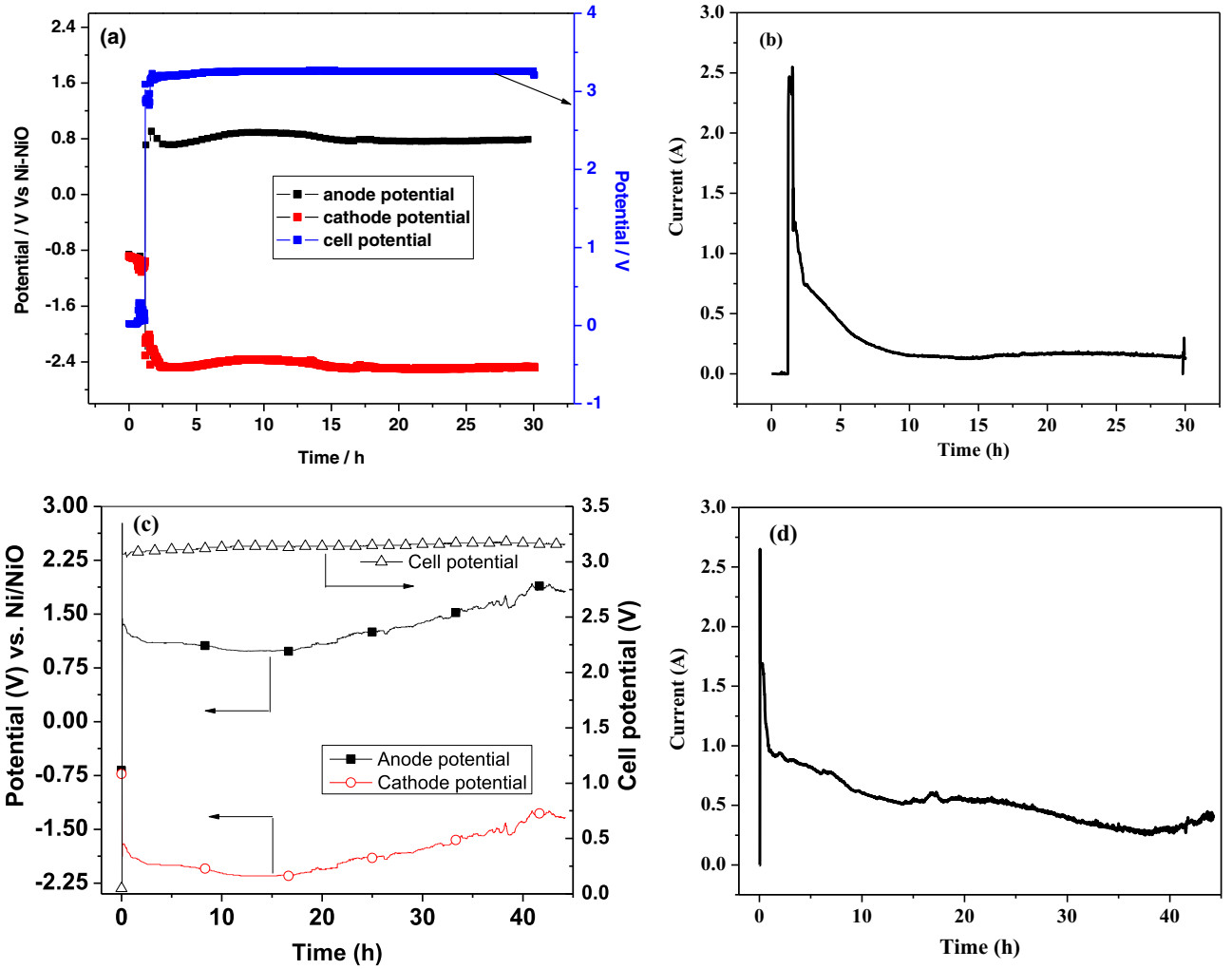

Figure 6. (a) The V-t curves of the UO_2 pellet electrode during electrolysis in LiCl-0.25 wt% Li_2O melt at 3.2 V and (b) the corresponding current behavior of the cell. Similar plots obtained in LiCl-1 wt.% Li_2O melt are shown in (c) and (d).

showed that the surface of the pellet alone was reduced to uranium metal but not the bulk (Fig. 5c). The SEM images of the fractured surface of the pellet before and after electrolysis are shown in Fig. 5d & 5e respectively. It is evident from the images that the surface morphology of the electrode was changed to that of uranium metal by electrolysis.

The experimental results confirm that UO_2 can be reduced to U metal in LiCl melt by electrons as proposed in the 'FFC Cambridge Process'. However, slow diffusion of oxygen toward the reaction interface will be a limiting factor in the reduction and this may warrant electrochemical deposition of lithium metal on the electrode at higher cathodic potentials and thus chemical reduction of the oxide to achieve acceptable rate of metal production for practical purposes.

Electro-reduction of UO_2 discs in LiCl-Li_2O melt.— Typical potential and current profiles of a similar cell as described above, but with LiCl-0.25wt.% Li_2O melt as the electrolyte, are shown in Fig. 6a and 6b respectively. The shapes of the I-t and V-t curves are more or less similar to those obtained in pure LiCl melt (Fig. 5a), but with the anode potential lowered by ~250 mV. It's interesting to note that a corresponding increase is registered in the cathodic potential too and the typical electrode behavior of the cell under constant voltage mode of electrolysis will be discussed in detail toward the later part of this section. As per the CV measurements mentioned previously, the anodic reaction 4 could commence from +0.75 V onwards and hence the observed anodic potential of ~ +0.77 V shows that the reaction 4 was occurring at the anode. XRD analysis showed that the surface of the electrolysed pellet was metallized. However, unlike in the case of the LiCl melt, carbon particles were seen dispersed in the used LiCl-0.25 wt% Li_2O melt.

The potential and current behavior of a UO_2 electro-reduction cell with LiCl containing 1 wt% Li_2O as the electrolyte melt and graphite rod anode are given in Fig. 6c and Fig. 6d, respectively. A comparison of the potential profiles with those of the previous two experiments reveals some striking features. The potential of the UO_2 cathode became more and more negative with time in both pure LiCl and LiCl-0.25 wt% Li_2O melts, but this was true only up to ~15 h of electrolysis (−1.75 V to −2.2 V) in the present melt and the trend was reversed for the remaining period of electrolysis. The XRD spectrum of the surface of the electrolysed pellet showed prominent lines of UO_2 and it confirmed that the surface was not completely reduced to U metal even after 45 h of electrolysis. However, electro-reduction of UO_2 in LiCl-1 wt% Li_2O with platinum anode has been established in many studies[7–13] and hence the difficulty in achieving complete reduction in the present case must be related to the use of graphite anode. As the surface reduction of the pellet could be achieved in both LiCl and LiCl-0.25wt.% Li_2O melts, the poor reduction in LiCl-1 wt% Li_2O must also be related to the higher concentration of Li_2O in the melt.

The typical electrode behavior of the cell can be explained as follows. It is seen from the CVs in Fig. 3 (curve b) and Fig. 4 that the

UO_2 to U reduction occurs at −2.18 V, i.e 180 mV positive to Li metal deposition on the electrode. No ternary intermediate compounds of the kind $Li_xU_yO_z$, were detected in the electrolysed product and hence the reduction is considered to occur by the reaction,

$$4Li^{+}_{(\text{in melt})} + UO_2 + 4e^- \rightarrow U + 2Li_2O_{(\text{in melt})} \quad [6]$$

A similar reaction was proposed by Vishnu et al. for electro-reduction of UO_2 in $CaCl_2$-42 wt% NaCl melt at 650°C.[35]

The CO_2 gas does not dissolve in LiCl melt and hence the CO_2 produced at the graphite anode as per reaction 4 escapes the electrode to the gas space of the reactor. However, when the melt contains Li_2O, carbon dioxide dissolves in the melt by the reaction,

$$O^{2-} + CO_2 \rightarrow {CO_3}^{2-} \quad [7]$$

The carbonate ions undergo cathodic reaction on an inert electrode as

$${CO_3}^{2-} + 4e^- \rightarrow C + 3O^{2-} \quad [8]$$

and an anodic reaction on a carbon electrode as

$$C + 2\,{CO_3}^{2-} \rightarrow 3\,CO_2 + 4e^- \quad [9]$$

It is evident from the above reactions that carbonate ions can be generated in an electro-deoxidation cell with LiCl-Li_2O melt electrolyte and graphite anode and these ions can be cathodically reacted to generate carbon in the melt. Obviously, the population of ${CO_3}^{2-}$ ions and the problems due to those will increase with increase in the Li_2O content of the melt. The stability of lithium carbonate, below 1000 K, in lithium chloride-lithium carbonate melt is reported high.[36]

Kruesi and Fray[37] reported that the cathodic reaction 8 at low carbonate concentrations in LiCl-Li_2CO_3 melts occurs at 1.2 V positive to that of Li deposition. Hur et al.[25] too reported the potential of reaction 8 as 1.226 V vs Li^+/Li in LiCl saturated Li_2O melts at 650°C. As discussed previously, the electro-reduction reaction 6 occurs at 180 mV positive to lithium deposition on the UO_2 electrode, which in turn means that the reaction 8 does take place along with reaction 6. In the present case, the cathode potential behavior of the cell up to ∼15 h (Fig. 6c) was similar to that of the cell with LiCl-0.25 wt% Li_2O melt (Fig. 6a) and this showed that the reaction 6 was occurring on the electrode in the beginning stages of the electrolysis. As electrolysis was continued, more and more carbonate ions were generated in the melt so that reaction 8 became the predominant cathodic reaction. As reaction 8 required lower energy than reaction 6, the cathodic potential became more anodic with time. In an electrolytic cell, working under constant applied voltage, the imposed voltage is distributed between the two electrodes and ohmic drop of the cell. Hence as the cathodic potential was decreased (became less negative), the anodic potential was increased by the same magnitude to maintain the constant applied voltage condition of the cell as shown by the V-t curves in Fig. 6c. The increase of the current toward the later part of electrolysis (Fig 6d) most probably is indicative of the increase in the concentration of the carbonate in the melt and its increased rate of discharge as per reaction 8. The graphite anode used in the electrolysis was found significantly thinned. A thick black deposit of carbon was found on the surface of the used salt (Fig. 7). Carbon was also found dispersed throughout the bulk of the salt, confirming thereby the occurrence of the cathodic reaction 8 in the cell. It is concluded from all these experimental results that though the presence of oxide ions in the melt is desirable for the electro-reduction of the oxide electrode, the reduction efficiency can be adversely affected by increase of the oxide content of the melt, when graphite is used as the anode.

Even as the conclusions are so drawn, it needs to be emphasized here that in the present electro-reduction experiments, the UO_2 cathode and graphite anode were kept very close in the melt and with no physical barrier provided in between. Also no shroud was provided around the graphite anode to guide the upward movement of carbon dioxide gas produced. In this kind of a simple cell configuration, the chances of dissolution of the carbon dioxide in the melt and its reaction with the oxide ions to form carbonate ions are high. It may be possible to mitigate the problems by proper design of the electro-reduction cell and use of optimized electrolyte composition. For example, the use of an oxide conducting membrane, which is compatible with the electrolyte melt, between the anode and cathode compartments of the cell might prevent formation of carbonate ions in the melt and thus the difficulties associated with the use of graphite anode.

Figure 7. Photographs of the used graphite anodes and the salt. Thick layer of carbon deposit is visible on the top of the salt, contained in the alumina crucible.

Summary

The studies on the electrochemical reduction of solid UO_2, carried out in LiCl-(0-1) wt% Li_2O melts with graphite anode have proved that the reduction of UO_2 to U is possible with graphite anode. The electro-reduction experiments carried out in conjunction with cyclic voltammetry of tantalum, graphite and UO_2 working electrodes, showed that the reduction occurred at potentials ∼180 mV positive to lithium deposition on the electrode by a probable reaction, $4Li^{+}_{(\text{in melt})} + UO_2 + 4e^- \rightarrow U + 2Li_2O_{(\text{in melt})}$. The experimental results show that the presence of small amounts of Li_2O in the electrolyte melt is a desirable factor in the reduction process, but the reduction can be adversely affected by a higher content of Li_2O in the melt owing to secondary reactions of the in-situ generated carbonate ions. The issue to a great extent could probably be addressed by proper design of the electro-reduction cell and by use of an optimized electrolyte composition. The results discussed in this preliminary study are indicative of the above prospects, but more detailed studies are necessary to arrive at the ideal electrolyte composition and appropriate cell design for efficient reduction of uranium oxide in LiCl-Li_2O melts with graphite anode.

Acknowledgments

The authors wish to express thanks to L. Shakila and V. Arunkumar for their help in the electro-reduction experiments.

References

1. T. Abram and S. Ion, *Energy Policy*, **36**, 4323 (2008).
2. J. J. Laidler, J. E. Battles, W. E. Miller, J. P. Ackerman, and E. L. Carls, *Prog. Nucl. Energy*, **31**, 131 (1997).
3. E. J. Karell, K. V. Gourishankar, J. L. Smith, L. S. Chow, and L. Redey, *Nucl. Technol.*, **136**, 342 (2001).
4. G. Z. Chen, D. J. Fray, and T. W. Farthing, *Nature*, **407**, 361 (2000).
5. K. S. Mohandas, *Trans. Inst. Min. Metall. C*, **122**, 195 (2013).
6. K. S. Mohandas and D. J. Fray, *Trans. Indian. Inst. Met.*, **57**, 579 (2004).
7. K. V. Gourishankar, L. Redey, and M. Williamson, Electrochemical reduction of metal oxides in molten salts, in *Light Metals*, Schneider, Editor, p. 1075, The Minerals, Metals and Materials Society, Warrendale, PA (2002).
8. S. M. Jeong, S. B. Park, S. S. Hong, C. S. Seo, and S. W. Park, *J. Radioanalytical. Nucl. Chem.*, **268**, 349 (2006).

9. C. S. Seo, S. B. Park, B. H. Park, K. J. Jung, S. W. Park, and S. H. Kim, *J. Nucl. Sci. and Technol.*, **43**, 587 (2006).
10. E. Y. Choi, J. M. Hur, I. K. Choi, S. G. Kwon, D. S. Kang, S. S. Hong, H. S. Shin, M. A. Yoo, and S. M. Jeong, *J. Nucl. Mater.*, **418**, 87 (2011).
11. E. Y. Choi, J. K. Kim, H. S. Im, I. K. Choi, S. H. Na, J. W. Lee, S. M. Jeong, and J. M. Hur, *J. Nucl. Mater.*, **437**, 178 (2013).
12. Y. Sakamura, M. Kurata, and T. Inoue, *J. Electrochem. Soc.*, **153**, D31 (2006).
13. J. M. Hur, S. S. Hong, and H. lee, *J. Radioanal. Nucl. Chem.*, **295**, 851 (2013).
14. Y. Sakamura, *J. Nucl. Mater.*, **412**, 177 (2011).
15. S. M. Jeong, H. S. Shin, S. H. Cho, J. M. Hur, and H. S. Lee, *Electrochim. Acta*, **54**, 6335 (2009).
16. E. Y. Choi, J. W. Lee, J. J. Park, J. M. Hur, J. K. Kim, K. Y. Jung, and S. M. Jeong, *Chem. Engg. J.*, **207–208**, 514 (2012).
17. T. Biju Joseph, N. Sanil, L. Shakila, K. S. Mohandas, and K. Nagarajan, *Electrochim. Acta*, **139**, 394 (2014).
18. S. Jiao and D. J. Fray, *Metall. Mater. Trans. B*, **41B**, 74 (2010).
19. T. Goto, Y. Araki, and R. Hagiwara, *Electrochem. Sol. State Lett.*, **9**, D5 (2006).
20. H. Yin, L. Gao, H. Zhu, X. Mao, F. Gan, and D. Wang, *Electrochim. Acta*, **56**, 3296 (2011).
21. K. T. Kilbi, S. Jiao, and D. J. Fray, *Electrochim. Acta*, **55**, 7126 (2010).
22. W. Park, J. K. Kim, J. M. Hur, E. Y. Choi, H. S. Im, and S. S. Hong, *J. Nucl. Mater.*, **432**, 175 (2013).
23. R. V. S. Nagesh, *DRDO Technology Spectrum*, 139–145, Desidoc Pub., New Delhi, 2012.
24. H. Y. Ryu, S. M. Jeong, Y. C. Kang, and J. G. Kim, *Asian Journal of Chemistry*, **25**, 7019 (2013).
25. J. M. Hur, J. S. Cha, and E. Y. Choi, *ECS Electrochemistry Letters*, **3**, E5 (2014).
26. M. Mohammedi, B. Borrenson, G. M. Harrberg, and R. Tunold, *J. Electrochem. Soc.*, **146**, 1472 (1999).
27. G. M. Harrberg, N. Aalberg, K. S. Osen, and R. Tunold in *Molten Salt Chemistry and Technology*, M. L. Saboungi, H. Kojima, J. Duruz, and D. Shores, Editors, p. 376, PV 93-9, The Electrochemical Society Proceedings Series, Pennington, NJ (1993).
28. T. Takenaka, M. Umehara, D. Araki, and T. Morishige, *ECS Transactions*, **50**, 127 (2012).
29. R. Tunold, G. M. Haarberg, K. S. Osen, A. M. Martinez, and E. Sandnes, *ECS Transactions*, **35**, 1 (2011).
30. D. S. Vishnu, N. Sanil, and L. Shakila,, G. Pannerselvam, R. Sudha, K. S. Mohandas, and K. Nagarajan, *Electrochim. Acta*, **100**, 51 (2013).
31. Roine: HSC Chemistry, version 5.1, Outokumpu Research, Oy, Pori, Finland, 2002.
32. K. S. Mohandas, N. Sanil, M. Noel, and P. Rodriguez, *J. Appl. Electrochem.*, **31**, 997 (2001).
33. K. S. Mohandas, L. Shakila, N. Sanil, D. S. Vishnu, and K. Nagarajan. Galvanostatic Studies on the Electro-deoxidation of Solid Titanium Dioxide in molten calcium chloride in *Molten Salts & Ionic Liquids*, Vol. 3, Florian Kongoli, Editor, p. 253, Proceedings of the FRAY International symposium on Metals and Materials Processing in a Clean Environment, Cancun, Mexico (2011).
34. J. M. Hur, S. M. Jeong, and H. Lee, *Electrochem. Commun.*, **12**, 706 (2010).
35. D. Sri Maha Vishnu, N. Sanil, G. Panneerselvam, R. Sudha, K. S. Mohandas, and K. Nagarajan, *J. Electrochem. Soc.*, **160**, D394 (2013).
36. R. Combes, R. Feys, and B. Tremellion, *J. Electrochem. Soc.*, **83**, 383 (1977).
37. W. H. Kruesi and D. J. Fray, *J. Appl. Electrochem.*, **24**, 1102 (1994).